

Fusing Pruned and Backdoored Models: Optimal Transport-based Data-free Backdoor Mitigation

Weilin Lin¹, Li Liu^{1*}, Jianze Li^{2,3}, Hui Xiong¹

¹The Hong Kong University of Science and Technology (Guangzhou)

²Shenzhen Research Institute of Big Data

³The Chinese University of Hong Kong, Shenzhen

Abstract

Backdoor attacks present a serious security threat to deep neuron networks (DNNs). Although numerous effective defense techniques have been proposed in recent years, they inevitably rely on the availability of either clean or poisoned data. In contrast, **data-free** defense techniques have evolved slowly and still lag significantly in performance. To address this issue, different from the traditional approach of pruning followed by fine-tuning, we propose a novel **data-free** defense method named *Optimal Transport-based Backdoor Repairing (OTBR)* in this work. This method, based on our findings on *neuron weight changes (NWCs)* of random unlearning, uses *optimal transport (OT)*-based model fusion to combine the advantages of both pruned and backdoored models. Specifically, we first demonstrate our findings that the NWCs of random unlearning are positively correlated with those of poison unlearning. Based on this observation, we propose a *random-unlearning NWC pruning* technique to eliminate the backdoor effect and obtain a backdoor-free pruned model. Then, motivated by the OT-based model fusion, we propose the *pruned-to-backdoored OT-based fusion* technique, which fuses pruned and backdoored models to combine the advantages of both, resulting in a model that demonstrates high clean accuracy and a low attack success rate. To our knowledge, this is the first work to introduce OT and model fusion techniques to the backdoor defense. Extensive experiments show that our method successfully defends against all seven backdoor attacks across three benchmark datasets, outperforming both state-of-the-art (SOTA) data-free and data-dependent methods.

Introduction

Over the past decade, deep neural networks (DNNs) have become a crucial technology in various applications, including image recognition (Parmar and Mehta 2014; He et al. 2016a), speech processing (Gaikwad, Gawali, and Yanawar 2010; Maas et al. 2017), and natural language processing (Chowdhary and Chowdhary 2020), *etc.* However, as the deployment of DNNs in sensitive and critical domains becomes more widespread, concerns regarding their security cannot be ignored. Among the numerous threats to DNNs, *backdoor attacks* (Gu et al. 2019; Li et al. 2021a; Wu et al. 2023) are particularly concerning. In these attacks, the attackers manipulate a small portion of the training data

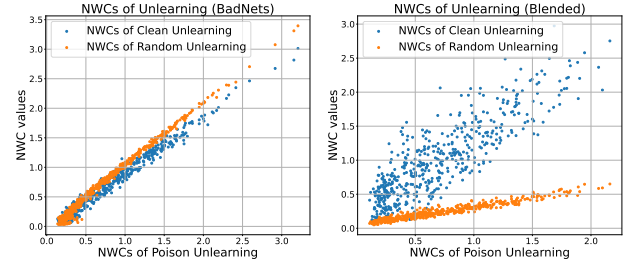


Figure 1: Illustration of unlearning NWCs on BadNets (Gu et al. 2019) and Blended (Chen et al. 2017) attacks. The NWCs of both clean and random unlearning show a positive correlation with poison unlearning. The last convolutional layer is chosen for this illustration.

to implant a stealthy backdoor into a DNN, resulting in a *backdoored model*. During inference, the backdoored model behaves anomalously when the input contains a pre-defined trigger pattern; otherwise, it performs normally. This phenomenon is termed the *backdoor effect*. Such attacks may pose hidden security issues to real-world applications, such as unauthorized access to a system when a company develops its software using a third-party pre-trained model.

In recent years, as backdoor attack methods have evolved, *backdoor defense* techniques have also seen significant growth. Various important techniques have been developed for backdoor defense, including pruning (Wu and Wang 2021), unlearning (Zeng et al. 2021a), and fine-tuning (Zhu et al. 2023), *etc.* However, most of these techniques rely on the availability of clean or poisoned data, which restricts their applicability to the aforementioned scenarios. Recent insights reveal a promising direction (Lin et al. 2024): using *neuron weight changes (NWCs)* of *clean unlearning*¹ to categorize the neurons into backdoor-related ones and clean ones², based on an observation that the NWCs of unlearning clean and poisoned data are positively correlated. In this work, our extended findings reveal that using random noise for unlearning, termed as *random unlearning*, brings a new similar insight: **the NWCs of random unlearning exhibit**

¹Unlearning the backdoored model on clean data.

²The larger NWC of a neuron, the more backdoor-related it is.

*Corresponds to Li Liu (avrillliu@hkust-gz.edu.cn)

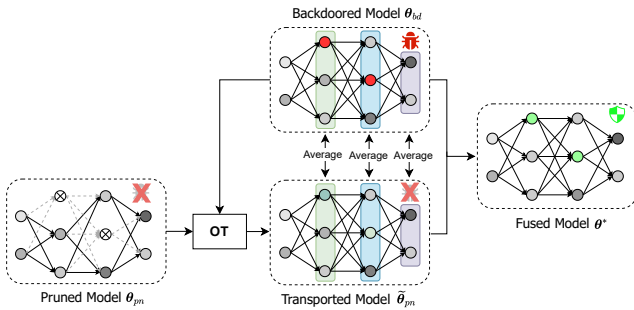


Figure 2: OT-based model fusion for backdoor defense. The pruned model is aligned with the backdoored model layer-by-layer using OT. Then the models are fused through a weighted averaging operation.

a **positive correlation with those of poison unlearning** (as shown in Figure 1). This motivates us to adopt NWCs for **data-free** backdoor mitigation using only the generated random noise. Normally, after identifying backdoor-related neurons, pruning (or zero reinitialization) followed by fine-tuning is employed to eliminate the backdoor effect and restore the lost performance (Liu, Dolan-Gavitt, and Garg 2018). However, this is infeasible in data-free scenarios since the subsequent fine-tuning requires clean data. If we only perform pruning using NWCs and simply skip the fine-tuning, the *clean accuracy* (ACC) is prone to decrease by more than 10% (Lin et al. 2024). Therefore, after pruning, it is necessary to develop a new data-free technique for performance recovery.

Recently, *model fusion* (Li et al. 2023a) has received increasing attention. It combines the weights of multiple models to integrate their capabilities into a single network. As one of the most representative works, OTFusion (Singh and Jaggi 2020) employs *optimal transport* (OT) to align model weights layer-by-layer before fusing two models through averaging. Following it, Intra-Fusion (Theus et al. 2024) employs OT to integrate the functionality of pruned neurons with the remaining ones, aiming to maintain great performance after pruning. It can be seen that the aforementioned methods both demonstrate OT’s inherent ability to preserve critical information during the fusion process.

Motivated by the above advancements in model fusion, in this work, we explore its potential to combine the high ACC of the backdoored model with the low *attack success rate* (ASR) of the pruned model in a data-free manner. Building on the foundation of NWC pruning and OT-based model fusion, we propose a novel data-free defense strategy called *Optimal Transport-based Backdoor Repairing* (OTBR), which fuses pruned and backdoored models. OTBR consists of two stages: *random-unlearning NWC pruning* and *pruned-to-backdoored OT-based fusion*. In the first stage, we calculate the NWCs based on random unlearning of the backdoored model, and then prune the top-ranking γ neurons to eliminate the backdoor effect. In the second stage, we align the weights of the pruned model with those of the backdoored model layer-by-layer using OT, and then fuse them into a single model. This process effectively

dilutes the backdoor effect while preserving the clean performance. An illustration of the fusion process is shown in Figure 2.

Our main contributions can be summarized as follows:

- We provide a new data-free pruning insight by revealing the positive correlation between NWCs when unlearning random noise and poisoned data.
- We propose a novel data-free defense strategy that combines the high ACC of the backdoored model with the low ASR of the pruned model, using the OT-based model fusion. To our knowledge, this is the first work to apply OT and model fusion techniques to backdoor defense.
- Experiments across various attacks, datasets, and experimental setups validate the effectiveness of our proposed OTBR method. Specifically, OTBR significantly outperforms both state-of-the-art (SOTA) data-free methods and SOTA data-dependent ones, consistently achieving successful defense performance against all tested attacks.

Related Work

Backdoor Attack

In the literature, various backdoor attacks on DNNs have been proposed, which can be generally categorized into two types: **data-poisoning attacks** and **training-controllable attacks**. For **data-poisoning attacks**, adversaries have access to the training dataset. BadNets (Gu et al. 2019), as one of the earliest examples, was proposed to implant a trigger pattern into the bottom-right corner of a small subset of the training images and reassign the labels to a specific target one. To enhance the stealthiness of the trigger, Blended (Chen et al. 2017) was proposed to blend the trigger onto the selected data with adjustable opacity. Recently, more sophisticated strategies have been proposed to enhance the trigger, including but not limited to SIG (Barni, Kallas, and Tondi 2019), label-consistent attacks (Shafahi et al. 2018; Zhao et al. 2020), and SSBA (Li et al. 2021a). Meanwhile, the second type, **training-controllable attacks**, is also rapidly evolving. In these attacks, adversaries have access to the training process, enabling more advanced attack strategies. Representative examples of this category include WaNet (Nguyen and Tran 2021) and Input-aware (Nguyen and Tran 2020), which incorporate an injection function into the training process to generate unique triggers for each input data. These innovative tactics make it more challenging to detect the triggers and conduct an effective defense.

Backdoor Defense

In general, backdoor defense methods can be categorized into three types³: pre-training, in-training, and post-training defenses. Among them, **Post-training Defense** has received the most attention, where the defenders aim to mitigate the backdoor effect of a well-trained backdoored model. FP (Liu, Dolan-Gavitt, and Garg 2018), as one of the

³As the first two categories are less related to the scenario in this paper, the details about them are postponed to the Appendix.

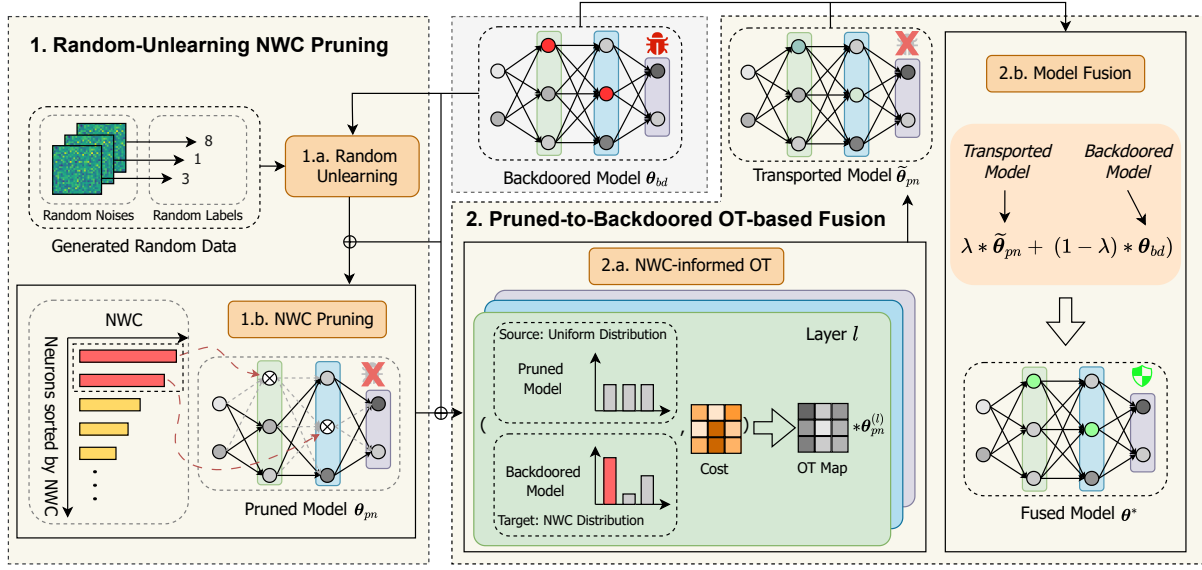


Figure 3: Overview of the proposed OTBR framework.

seminal defense methods, prunes the less-activated neurons and then fine-tunes the model, based on the observation that poisoned and clean data activate different neurons; ANP (Wu and Wang 2021) detects and prunes backdoor-related neurons by applying adversarial perturbations to neuron weights; Building on this, RNP (Li et al. 2023b) refines the perturbation technique using clean unlearning, and performs pruning based on a learned mask. Except for these pruning-based techniques, there also exist some other important defense techniques. For instance, NC (Wang et al. 2019) proposes recovering the trigger to improve backdoor removal; NAD (Li et al. 2021c) pioneers the use of model distillation to train a benign student model; i-BAU (Zeng et al. 2021a) uses adversarial attacks to identify potential triggers and then performs poison unlearning to mitigate the backdoor effect.

Different from the above defenses, which are all data-dependent, CLP (Zheng et al. 2022) is the first data-free defense method, which identifies and prunes potential backdoored neurons based on channel Lipschitzness; ABD (Hong et al. 2023) designs a plug-in defensive technique specialized for data-free knowledge distillation; DHBE (Yan et al. 2023) proposes a competing strategy between distillation and backdoor regularization to distill a clean student network without data.

Although several data-dependent techniques have already been proposed in the literature, the scarcity of data-free defense techniques still limits the applicability of backdoor defenses in real-world scenarios. In this paper, we will focus on addressing this issue, and develop a novel effective data-free defense method by using random-unlearning NWCs and the OT-based model fusion technique.

Preliminary

Threat Model

In this work, we address threats from both data-poisoning and training-controllable attacks. The attackers aim to poison a small portion of the training data so that the trained model predicts a target class when presented with data containing a pre-defined *trigger*, while otherwise performing normally. The weights of a L -layer backdoored model are denoted as $\theta_{bd} = \{\theta_{bd}^{(l)}\}_{1 \leq l \leq L}$, where $\theta_{bd}^{(l)}$ represents the weights for the l^{th} layer, consisting of $m^{(l)}$ neurons.

Defense Setting

We focus on the post-training scenario, aiming to mitigate the backdoor effect of a well-trained backdoored model while minimizing the negative impact on ACC. Different from most previous works (Liu, Dolan-Gavitt, and Garg 2018; Wu and Wang 2021; Zeng et al. 2021a), which assumes access to 5% of clean data for defense, we adopt a more stringent approach that relies only on the backdoored model, without access to any clean data (Zheng et al. 2022).

Method

Overview of Our Method

The complete data-free defense process of our proposed OTBR strategy is illustrated in Figure 3, which consists of two stages as follows:

- In **Stage 1**, referred to as *random-unlearning NWC pruning*, we aim to obtain a backdoor-free model. Specifically, we first conduct random unlearning on the backdoored model for I iterative steps. During each step, a mini-batch of random noise with random labels is generated and used for unlearning. Then, we calculate the NWC for each neuron based on their weights from both

the original backdoored and unlearned models. Finally, we prune the top-ranking γ of neurons, based on their NWCs, from the backdoored model to eliminate its backdoor effect.

- In **Stage 2**, referred to as *pruned-to-backdoored OT-based fusion*, when obtaining a sub-optimal pruned model, we aim to combine its low ASR with the high ACC of the original backdoored model by repairing the backdoor-related neurons using OT-based model fusion. Specifically, we propose *NWC-informed OT* to align the weights of the pruned model with those of the backdoored model layer-by-layer, taking into account the backdoor importance as determined by NWCs. For each layer, starting with the earliest pruned one, we initialize the probability mass on neuron weights using a uniform distribution for the pruned model and an NWC distribution for the original backdoored model. This strategy discriminatively transfers clean functionality to the backdoor-related neurons. The cost matrix $\mathbf{C}^{(l)}$ is calculated based on the Euclidean distance between neuron weights from the two models. Using this cost matrix, we then derive the optimal transport map $\mathbf{T}^{(l)}$ and employ it to transport the weights of the pruned model. After aligning all layers, we perform a simple weight averaging to fuse the transported and backdoored models, resulting in an effective defense.

Next, we will present more detailed formulations and provide further insights.

Stage 1: Random-Unlearning NWC Pruning

Random Unlearning. Unlearning is a reverse training process designed to maximize the loss value on a given dataset (Li et al. 2023b). In this work, we define *random unlearning* as the process of unlearning a DNN model f using a generated random dataset \mathcal{D}_r . More precisely, random unlearning on the backdoored model θ_{bd} is formulated as:

$$\max_{\theta_{bd}} \mathbb{E}_{(\mathbf{x}_r, y_r) \in \mathcal{D}_r} [\mathcal{L}(f(\mathbf{x}_r; \theta_{bd}), y_r)], \quad (1)$$

where the loss function \mathcal{L} is chosen to be a cross-entropy loss, and the generated random dataset \mathcal{D}_r contains $I \times B$ pairs of random noises $\mathbf{x}_r \in [0, 1]^{A \times H \times W}$ and random labels $y_r \in \{0, 1, \dots, G\}$. Here, I is the number of iterative steps; B is the batch size; A , H and W represent the generated noise size; and G is the largest class label.

NWC Pruning. We follow the NWC definition from (Lin et al. 2024) to quantify the weight changes for each neuron during unlearning. Specifically, for the j -th neuron in the l -th layer, the NWC is defined as:

$$\text{NWC}^{(l)j} \stackrel{\text{def}}{=} \|\theta_{ul}^{(l)j} - \theta_{bd}^{(l)j}\|_1, \quad (2)$$

where θ_{ul} denotes the unlearned backdoored model, $j \in \{1, \dots, m^{(l)}\}$ and $l \in \{1, \dots, L\}$. To eliminate the backdoor effect, we sort all calculated NWCs in descending order and prune the top-ranking γ of neurons from the original backdoored model. The pruned model is denoted as θ_{pn} .

To better understand why substituting clean unlearning with random unlearning is effective for NWC pruning, we

provide a possible explanation in the **Further Analysis of Appendix**.

Stage 2: Pruned-to-Backdoored OT-based Fusion

Optimal Transport. OT is a mathematical framework to find the most economical way to transport mass from one distribution to another. Suppose we have two discrete probability distributions in the space $\mathcal{X} = \{x_i\}_{i=1}^n$ and $\mathcal{Y} = \{y_j\}_{j=1}^m$, i.e., the source distribution $\mu := \sum_{i=1}^n \alpha_i \cdot \delta(x_i)$ and the target distribution $\nu := \sum_{j=1}^m \beta_j \cdot \delta(y_j)$, where $\sum_{i=1}^n \alpha_i = \sum_{j=1}^m \beta_j = 1$ and $\delta(\cdot)$ is the Dirac delta function. The OT problem can be formulated as a linear programming problem as follows:

$$\begin{aligned} \text{OT}(\mu, \nu; \mathbf{C}) &\stackrel{\text{def}}{=} \min \langle \mathbf{T}, \mathbf{C} \rangle, \\ \text{s.t., } \mathbf{T} \mathbf{1}_m &= \boldsymbol{\alpha}, \quad \mathbf{T}^\top \mathbf{1}_n = \boldsymbol{\beta}, \end{aligned} \quad (3)$$

where $\mathbf{T} \in \mathbb{R}_+^{n \times m}$ is the transport map that determines the optimal transport amount of mass from \mathcal{X} to \mathcal{Y} , and \mathbf{C} is the cost matrix quantifying the cost of moving each unit of mass.

NWC-informed OT. In our approach, we align the NWC-pruned model, which contains only clean functionality, with the original backdoored model to achieve more effective fusion. The goal is to dilute the backdoor effect with the least influence on clean performance. To achieve this, we focus more on the backdoor-related neurons during weight transport by employing NWC-informed initialization for the target distribution ν (backdoored model), while using a uniform distribution for the source distribution μ (pruned model). For the l -th layer, we denote the probability mass as:

$$\boldsymbol{\alpha}^{(l)} \stackrel{\text{def}}{=} \left\{ \frac{1}{n^{(l)}} \right\}_{i=1}^{n^{(l)}}, \quad \boldsymbol{\beta}^{(l)} \stackrel{\text{def}}{=} \left\{ \frac{\text{NWC}^{(l)j}}{\sum_{j=1}^{m^{(l)}} \text{NWC}^{(l)j}} \right\}_{j=1}^{m^{(l)}}, \quad (4)$$

where $n^{(l)}$ and $m^{(l)}$ denote the neuron numbers of pruned and backdoored models, respectively. Then, based on the distributions $\mu^{(l)}$ and $\nu^{(l)}$, and the cost matrix $\mathbf{C}^{(l)}$, we can derive the optimal transport map $\mathbf{T}^{(l)}$ by equation (3).

Model Fusion. Inspired by the OTFusion (Singh and Jaggi 2020), we align and fuse the pruned and backdoored models layer-by-layer, using OT in equation (3) and our defined distributions in equation (4). The details of the entire fusion process are shown in Algorithm 1. Note that we start the fusion process from the first pruned layer p , rather than the second layer. For the l -th layer, $n^{(l)}$ and $m^{(l)}$ represent the neuron number of $\theta_{pn}^{(l)}$ and $\theta_{bd}^{(l)}$, respectively.

In Algorithm 1, for each layer l , we first align the incoming edge weights using the OT map $\mathbf{T}^{(l-1)}$ and probability mass $\boldsymbol{\beta}^{(l-1)}$ from the previous layer:

$$\hat{\theta}_{pn}^{(l)} \leftarrow \theta_{pn}^{(l)} \mathbf{T}^{(l-1)} \text{diag}(1/\boldsymbol{\beta}^{(l-1)}).$$

Then, we get the distributions $\mu^{(l)}$ and $\nu^{(l)}$ of the current layer and compute the cost matrix $\mathbf{C}^{(l)}$ using Euclidean distance between neuron weights: $\mathbf{C}_{ij}^{(l)} \stackrel{\text{def}}{=} \|\theta_{pn}^{(l)i} - \theta_{bd}^{(l)j}\|^2$.

Algorithm 1: Pruned-to-Backdoored OT-based Fusion

Input: Pruned model θ_{pn} , backdoored model θ_{bd} , random-unlearning NWC values for each neuron, balance coefficient λ , the first pruned layer p .
Output: Clean model θ^* .

```

1:  $\alpha^{(p-1)} \leftarrow \{1/n^{(p-1)}\}_{i=1}^{n^{(p-1)}}$ 
    $\beta^{(p-1)} \leftarrow \{1/m^{(p-1)}\}_{j=1}^{m^{(p-1)}}$ 
2:  $\mathbf{T}^{(p-1)} \leftarrow \text{diag}(\beta^{(p-1)}) \mathbf{I}_{m^{(p-1)} \times m^{(p-1)}}$ 
3: for  $l = p$  to  $L$  do
4:    $\hat{\theta}_{pn}^{(l)} \leftarrow \theta_{pn}^{(l)} \mathbf{T}^{(l-1)} \text{diag}(1/\beta^{(l-1)})$ 
5:    $\alpha^{(l)} \leftarrow \{1/n^{(l)}\}_{i=1}^{n^{(l)}}$ 
6:    $\beta^{(l)} \leftarrow \left\{ \text{NWC}^{(l)j} / \sum_{j=1}^{m^{(l)}} \text{NWC}^{(l)j} \right\}_{j=1}^{m^{(l)}}$ 
7:    $\mu^{(l)}, \nu^{(l)} \leftarrow \text{GetDistribution}(\alpha^{(l)}, \beta^{(l)})$ 
8:    $\mathbf{C}^{(l)} \leftarrow \text{ComputeCost}(\theta_{pn}^{(l)}, \theta_{bd}^{(l)})$ 
9:    $\mathbf{T}^{(l)} \leftarrow \text{OT}(\mu^{(l)}, \nu^{(l)}, \mathbf{C}^{(l)})$ 
10:   $\tilde{\theta}_{pn}^{(l)} \leftarrow \text{diag}(1/\beta^{(l)}) \mathbf{T}^{(l)\top} \hat{\theta}_{pn}^{(l)}$ 
11:   $\theta^{*(l)} \leftarrow \lambda \tilde{\theta}_{pn}^{(l)} + (1 - \lambda) \theta_{bd}^{(l)}$ 
12: end for
13: Obtain clean model  $\theta^*$ 

```

Finally, as in equation (3), using $\mu^{(l)}$, $\nu^{(l)}$ and $\mathbf{C}^{(l)}$, the OT map $\mathbf{T}^{(l)}$ of the current layer can be derived, and the transported pruned model $\tilde{\theta}_{pn}^{(l)}$ can be obtained as:

$$\tilde{\theta}_{pn}^{(l)} \leftarrow \text{diag}\left(1/\beta^{(l)}\right) \mathbf{T}^{(l)\top} \hat{\theta}_{pn}^{(l)},$$

which has been aligned with the backdoored model.

After alignment, the transported model is then fused with the backdoored model to obtain the final defense model, which can be formulated as:

$$\theta^* \leftarrow \lambda \tilde{\theta}_{pn} + (1 - \lambda) \theta_{bd},$$

where θ^* represents the fused clean model and λ is the balance coefficient.

Why Can OT-based Fusion Mitigate Backdoor Effect?

We now offer a possible explanation for the effectiveness of OT-based model fusion in mitigating backdoor effects. Based on previous work (Lin et al. 2024), the NWC-pruned model can be made backdoor-free, *i.e.*, the ASR dropping to zero, by selecting a suitable pruning threshold. Therefore, by aligning the pruned model with the original backdoored model using NWC-informed OT, we can transport the clean functionality of the remaining neurons to the nearest backdoored positions, as determined by NWCs and Euclidean distance. Then, further fusion based on the transported model can be viewed as a dilution operation to weaken the backdoored effect of the original backdoored model while preserving its clean functionality, thanks to the inherent ability of OT (Singh and Jaggi 2020; Theus et al. 2024). This is consistent with the previous insights that the

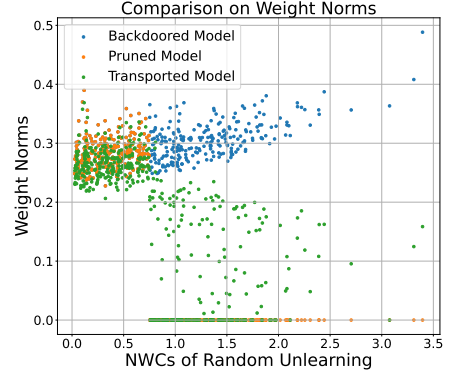


Figure 4: Illustration of neuron-level weight norms for the backdoored, pruned, and transported models during OT-based fusion.

backdoor task is easier and encoded in much fewer neurons than the clean task (Li et al. 2021b; Cai et al. 2022).

A practical example of the BadNets-attacked PreAct-ResNet18 (He et al. 2016b) is illustrated in Figure 4. From the perspective of *weight norm*, the larger the difference in a neuron’s weight between the pruned and transported models, the more it is transported by the OT. We observe a consistent, slight decrease in the unpruned neurons that are intensively transported to some specific pruned neurons, resulting in their rapid recovery. This outcome reflects the effect of transporting from a uniform source distribution to a NWC-informed target distribution. By fusing the transported (green) and backdoored (blue) models, we can discriminately modify the neuron functionality, *e.g.*, recovering more in low-NWC neurons, to effectively mitigate the backdoor effect while preserving high performance. More observations on activations are provided in the **Further Analysis of Appendix**.

Experiment

Experimental Setup

For a fair comparison, all experiments, including the code implementation of our proposed method, are conducted using the default settings in BackdoorBench (Wu et al. 2022).

Datasets. Similar to previous works (Zhu et al. 2023; Wei et al. 2023), our experiments are conducted on three benchmark datasets, including CIFAR-10 (Krizhevsky, Hinton et al. 2009), Tiny ImageNet (Le and Yang 2015), and CIFAR-100 (Krizhevsky, Hinton et al. 2009).

Attack Setup. We evaluate the effectiveness of all defense methods using seven SOTA backdoor attacks: BadNets (Gu et al. 2019), Blended (Chen et al. 2017), Input-aware (Nguyen and Tran 2020), LF (Zeng et al. 2021b), SSBA (Li et al. 2021a), Trojan (Liu et al. 2018) and WaNet (Nguyen and Tran 2021). All attacks are conducted using the default settings in BackdoorBench (Wu et al. 2022). For example, we set the target label to 0, the poi-

Table 1: Performance comparison with the SOTA defenses on CIFAR-10, Tiny ImageNet, and CIFAR-100 (%).

Datasets	Attacks	No Defense		Data-Dependent										Data-Free			
				FP		NAD		ANP		i-BAU		RNP		CLP		OTBR	
		ACC	ASR	ACC	ASR	ACC	ASR	ACC	ASR	ACC	ASR	ACC	ASR	ACC	ASR	ACC	ASR
CIFAR-10	BadNets	91.32	95.03	91.31	57.13	89.87	2.14	90.94	5.91	89.15	1.21	89.81	24.97	90.06	77.50	90.11	1.08
	Blended	93.47	99.92	93.17	99.26	92.17	97.69	93.00	84.90	87.00	50.53	88.76	79.74	91.32	99.74	92.01	1.64
	Input-aware	90.67	98.26	91.74	0.04	93.18	1.68	91.04	1.32	89.17	27.08	90.52	1.84	90.30	2.17	86.52	0.37
	LF	93.19	99.28	92.90	98.97	92.37	47.83	92.83	54.99	84.36	44.96	88.43	7.02	92.84	99.18	87.68	9.69
	SSBA	92.88	97.86	92.54	83.50	91.91	77.40	92.67	60.16	87.67	3.97	88.60	17.89	91.38	68.13	85.27	9.54
	Trojan	93.42	100.00	92.46	71.17	91.88	3.73	92.97	46.27	90.37	2.91	90.89	3.59	92.98	100.00	90.62	7.50
	WaNet	91.25	89.73	91.46	1.09	93.17	22.98	91.32	2.22	89.49	5.21	90.43	0.96	81.91	78.42	88.12	10.93
	Average	92.31	97.15	92.23	58.74	92.08	36.21	92.11	36.54	88.17	19.41	89.63	19.43	90.11	75.02	88.62	5.82
Tiny ImageNet	BadNets	56.23	100.00	51.73	99.99	46.37	0.27	50.55	7.74	51.48	97.36	21.91	0.00	55.94	100.00	54.13	0.00
	Input-aware	57.45	98.85	55.28	62.92	47.91	1.86	53.17	0.17	52.48	72.98	15.57	0.00	57.75	99.58	51.40	0.02
	SSBA	55.22	97.71	50.47	88.87	45.32	57.32	52.83	91.44	49.86	81.90	37.64	0.00	55.17	97.65	54.15	3.89
	Trojan	55.89	99.98	50.22	8.82	48.48	0.83	50.37	1.40	52.65	98.49	46.27	0.00	55.86	8.39	53.85	0.14
	WaNet	56.78	99.49	53.84	3.94	46.98	0.43	53.87	0.75	53.71	75.23	20.50	0.00	56.21	98.50	55.64	0.03
	Average	56.31	99.21	52.31	52.91	47.01	12.14	52.16	20.30	52.04	85.19	28.38	0.00	56.19	80.82	53.83	0.82
CIFAR-100	BadNets	67.22	87.43	64.55	0.42	66.37	0.06	63.65	0.00	60.37	0.04	55.68	0.00	65.40	81.95	66.81	0.00
	Input-aware	65.24	98.61	67.82	2.34	69.25	31.11	58.99	0.00	65.21	85.14	55.66	0.01	65.22	99.81	59.64	4.21
	SSBA	69.06	97.22	61.60	14.02	67.38	89.51	64.35	39.60	63.09	28.91	68.44	92.80	65.39	97.52	66.89	1.28
	WaNet	64.04	97.72	68.07	10.29	68.46	0.55	60.05	0.05	65.31	43.96	49.48	0.00	25.90	83.49	62.91	8.18
	Average	66.39	95.25	65.51	6.77	67.87	30.31	61.76	9.91	63.50	39.51	57.32	23.20	55.48	90.69	64.06	3.42
Average ACC Drop (smaller is better)				↓1.51	-	↓2.64	-	↓2.55	-	↓3.87	-	↓12.17	-	↓3.73	-	↓2.97	-
Average ASR Drop (larger is better)				-	↓53.39	-	↓70.11	-	↓72.51	-	↓52.33	-	↓83.02	-	↓16.57	-	↓93.66
Successful Defense Count				8 / 16		9 / 16		10 / 16		5 / 16		7 / 16		2 / 16		16 / 16	

soning ratio to 10%, and the tested model to PreAct-ResNet18 (He et al. 2016b).

Defense Setup. We compare our proposed OTBR method with six SOTA defense methods: Fine-pruning (FP) (Liu, Dolan-Gavitt, and Garg 2018), NAD (Li et al. 2021c), ANP (Wu and Wang 2021), i-BAU (Zeng et al. 2021a), RNP (Li et al. 2023b), and CLP (Zheng et al. 2022). Note that only CLP can be conducted in a data-free manner similar to OTBR, while the other five defenses are all data-dependent. Therefore, we follow the common setting in the post-training scenario that 5% clean data is provided for those methods. Due to space limit, more detailed settings regarding our method are postponed to the **Implementation Details of Appendix**.

Evaluation Metrics. We use two common metrics to evaluate performance: ACC and ASR. They measure the proportion of correct predictions on clean data (the higher, the better) and the rate of incorrect predictions for the target label on poisoned data (the lower, the better), respectively. A defense is usually considered successful against an attack if the ASR is reduced to below 20% (Qi et al. 2023; Xie et al. 2024). In this paper, to consider both ACC and ASR, we consider a defense to be **successful** (marked with green in all tables) only if it achieves both of the following criteria: ACC decreases by less than 10% and ASR falls below 20%. Otherwise, it is considered unsuccessful. The best average results are **boldfaced** in all tables within this section.

Compared with Previous Works

The main defense performance, compared with the six baseline methods, is shown in Table 1. We observe that our OTBR successfully defends against all 16 attacks across three benchmark datasets, achieving the largest drop in average ASR (93.66%) with an acceptable average ACC reduction (2.97%). Moreover, OTBR outperforms both data-free and data-dependent defenses, achieving the lowest av-

Table 2: Comparison of different fusion schemes on CIFAR-10 (%). V_1 : no fusion; V_2 : vanilla fusion; V_3 : OT-based fusion.

Attacks	V_1		V_2		V_3 (Ours)	
	ACC	ASR	ACC	ASR	ACC	ASR
BadNets	84.98	1.56	91.3	81.13	90.11	1.08
Blended	69.08	4.71	92.06	16.76	92.01	1.64
LF	54.15	0.83	90.97	60.4	87.68	9.69
SSBA	40.58	0.02	89.84	40.57	85.27	9.54

erage ASR on CIFAR-10 and CIFAR-100, and the second-best ASR on Tiny ImageNet. Notably, the best ASR on Tiny ImageNet, achieved by RNP, comes with a significant drop in ACC. For the performances of baseline methods, we observe that the data-dependent approaches have clear advantages over the data-free CLP, which succeeds in only 2 out of 16 defenses. ANP achieves the best results with 10 out of 16 successful defenses; however, it consistently fails against SSBA attacks, a shortcoming also observed in NAD. Despite its failures on CIFAR-10, FP performs well on CIFAR-100 and consistently achieves high ACCs across all three datasets, validating the effectiveness of fine-tuning. i-BAU fails completely on Tiny ImageNet, exposing its limitations when dealing with different data complexities. Although RNP achieves good performance in ASR, it fails with significant drops in ACC on Tiny ImageNet. In contrast, OTBR performs the best, consistently achieving superior results across various attacks and datasets. For a comprehensive evaluation, we also discuss the computational cost, the impact of different poisoning ratios, and the performance on different models in the **More Experiments of Appendix**.

Ablation Studies

Effectiveness of OT-based Model Fusion. To evaluate the effectiveness of OT-based model fusion, we keep Stage 1 unchanged and modify Stage 2 to generate three different

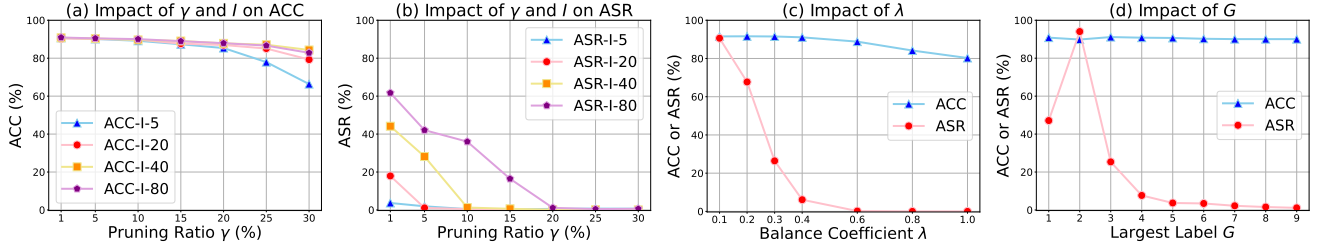


Figure 5: Impact of different factors on performance. (a) and (b) show the impact of γ and I on ACC and ASR, respectively, with “ACC-I-5” representing ACC when $I = 5$; (c) shows the impact of λ ; and (d) shows the impact of G .

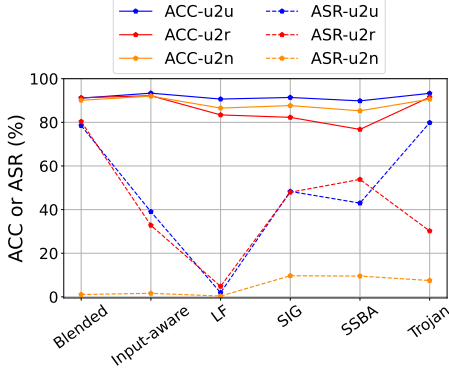


Figure 6: Comparison of different OT distributions. u2u: uniform to uniform transport; u2r: uniform to random transport; u2n(ours): uniform to NWC transport.

versions for comparison. (1) V_1 : no fusion is conducted in Stage 2; instead, we evaluate the performance of the pruned model from Stage 1; (2) V_2 : implement vanilla fusion by directly fusing the pruned model with the backdoored model using equation (); (3) V_3 (Ours): the final version, where the full procedures of both Stage 1 and 2 are conducted. Table 2 shows the performances of these three versions on CIFAR-10 across four different attacks. The results validate the effectiveness of aligning neuron weights using OT, where the pruned model inherently achieves a low ASR (or even better) while the high ACC is kept. Although the vanilla fusion (V_2) better preserves ACC, it fails in effectively mitigating the backdoor effect.

Effectiveness of NWC-informed OT. We now further verify the important role of NWC-informed OT in achieving optimal defense performance. To do this, we fix the source distribution as a uniform distribution and compare three different initialization schemes for the target distribution in OT. Specifically, we consider three types of distributions: *uniform distribution*, *random distribution*, and *NWC distribution*. These schemes are labeled as “u2u”, “u2r”, and “u2n”(Ours), respectively. The results are presented in Figure 6. We observe that only “u2n”, *i.e.*, NWC-informed OT, consistently achieves strong performance across different attacks. In contrast, uniform and random distributions fail to effectively guide neuron weight transport, resulting in poor

fusion performance.

Parameter Analysis

Impact of Different Factors. We aim to investigate the impact of various factors on the performance of OTBR. These factors include the number of iterative steps I , the pruning ratio γ , the largest label G , and the balance coefficient λ . The experiments are conducted using default settings on CIFAR-10 and BadNets with a 10% poisoning ratio. The results are shown in Figure 5. **Firstly**, in subfigures (a) and (b), we present the results of varying the pruning ratio γ from 1% to 30% across four numbers of iterative steps I (5, 20, 40, and 80 steps). The two subfigures, showing ACC and ASR respectively, demonstrate that OTBR performs well across different settings. A larger pruning ratio tends to require more iterative steps for effective random unlearning. In our setting ($I = 20$), γ is insensitive in the range of 5% to 25%, resulting in successful defense. **Secondly**, in subfigure (c), we show the impact of the balance coefficient λ ranging from 0.1 to 1.0. A higher value of λ means a more important role the transported model plays in the fusion. We observe that there exists a trade-off between the high ACC from the backdoored model and the low ASR from the transported model, as we assumed before. It suggests setting the λ between 0.4 and 0.8 for a successful defense. **Lastly**, in subfigure (d), we evaluate the performances with different largest labels G for random data generation to test the impact of class number. Note that 9 is the largest label, in which case the model is trained. The results reveal that performance remains consistently good across G values from 4 to 9, while a smaller class number may fail. Overall, our OTBR proves to be a robust defense method across various hyperparameter settings.

Conclusion

In this work, we propose a novel data-free backdoor defense method, OTBR, using OT-based model fusion. Notably, we provide a new data-free pruning insight by revealing the positive correlation between NWCs when unlearning random noise and poisoned data. This insight enables us to effectively eliminate the backdoor effect using pruning guided by NWCs in a data-free manner. Then, we propose to combine the high ACC of the backdoored model with the low ASR of the pruned model using the OT-based model fusion. Furthermore, we provide possible explanations for the suc-

cess of both NWC pruning and OT-based fusion. Extensive experiments across various attacks and datasets confirm the effectiveness of our OTBR method. A current limitation of this work is its reliance on NWC, which applies only to the post-training scenario. In future work, we plan to explore the potential of OT-based model fusion for more scenarios, such as in-training defense.

References

- Barni, M.; Kallas, K.; and Tondi, B. 2019. A new backdoor attack in cnns by training set corruption without label poisoning. In *2019 IEEE International Conference on Image Processing (ICIP)*, 101–105. IEEE.
- Cai, R.; Zhang, Z.; Chen, T.; Chen, X.; and Wang, Z. 2022. Randomized channel shuffling: Minimal-overhead backdoor attack detection without clean datasets. *Advances in Neural Information Processing Systems*, 35: 33876–33889.
- Chen, B.; Carvalho, W.; Baracaldo, N.; Ludwig, H.; Edwards, B.; Lee, T.; Molloy, I.; and Srivastava, B. 2018. Detecting backdoor attacks on deep neural networks by activation clustering. *arXiv preprint arXiv:1811.03728*.
- Chen, W.; Wu, B.; and Wang, H. 2022. Effective backdoor defense by exploiting sensitivity of poisoned samples. *Advances in Neural Information Processing Systems*, 35: 9727–9737.
- Chen, X.; Liu, C.; Li, B.; Lu, K.; and Song, D. 2017. Targeted backdoor attacks on deep learning systems using data poisoning. *arXiv preprint arXiv:1712.05526*.
- Chowdhary, K.; and Chowdhary, K. 2020. Natural language processing. *Fundamentals of artificial intelligence*, 603–649.
- Gaikwad, S. K.; Gawali, B. W.; and Yannawar, P. 2010. A review on speech recognition technique. *International Journal of Computer Applications*, 10(3): 16–24.
- Gu, T.; Liu, K.; Dolan-Gavitt, B.; and Garg, S. 2019. Badnets: Evaluating backdooring attacks on deep neural networks. *IEEE Access*, 7: 47230–47244.
- He, K.; Zhang, X.; Ren, S.; and Sun, J. 2016a. Deep residual learning for image recognition. In *Proceedings of the IEEE conference on computer vision and pattern recognition*, 770–778.
- He, K.; Zhang, X.; Ren, S.; and Sun, J. 2016b. Identity mappings in deep residual networks. In *Computer Vision—ECCV 2016: 14th European Conference, Amsterdam, The Netherlands, October 11–14, 2016, Proceedings, Part IV 14*, 630–645. Springer.
- Hong, J.; Zeng, Y.; Yu, S.; Lyu, L.; Jia, R.; and Zhou, J. 2023. Revisiting data-free knowledge distillation with poisoned teachers. In *International Conference on Machine Learning*, 13199–13212. PMLR.
- Huang, K.; Li, Y.; Wu, B.; Qin, Z.; and Ren, K. 2022. Backdoor defense via decoupling the training process. *arXiv preprint arXiv:2202.03423*.
- Krizhevsky, A.; Hinton, G.; et al. 2009. Learning multiple layers of features from tiny images.
- Le, Y.; and Yang, X. 2015. Tiny imagenet visual recognition challenge. *CS 231N*, 7(7): 3.
- Li, W.; Peng, Y.; Zhang, M.; Ding, L.; Hu, H.; and Shen, L. 2023a. Deep model fusion: A survey. *arXiv preprint arXiv:2309.15698*.
- Li, Y.; Li, Y.; Wu, B.; Li, L.; He, R.; and Lyu, S. 2021a. Invisible backdoor attack with sample-specific triggers. In *Proceedings of the IEEE/CVF international conference on computer vision*, 16463–16472.
- Li, Y.; Lyu, X.; Koren, N.; Lyu, L.; Li, B.; and Ma, X. 2021b. Anti-backdoor learning: Training clean models on poisoned data. *Advances in Neural Information Processing Systems*, 34: 14900–14912.
- Li, Y.; Lyu, X.; Koren, N.; Lyu, L.; Li, B.; and Ma, X. 2021c. Neural attention distillation: Erasing backdoor triggers from deep neural networks. *arXiv preprint arXiv:2101.05930*.
- Li, Y.; Lyu, X.; Ma, X.; Koren, N.; Lyu, L.; Li, B.; and Jiang, Y.-G. 2023b. Reconstructive neuron pruning for backdoor defense. In *International Conference on Machine Learning*, 19837–19854. PMLR.
- Lin, W.; Liu, L.; Wei, S.; Li, J.; and Xiong, H. 2024. Unveiling and Mitigating Backdoor Vulnerabilities based on Unlearning Weight Changes and Backdoor Activeness. *arXiv preprint arXiv:2405.20291*.
- Liu, K.; Dolan-Gavitt, B.; and Garg, S. 2018. Fine-pruning: Defending against backdooring attacks on deep neural networks. In *International symposium on research in attacks, intrusions, and defenses*, 273–294. Springer.
- Liu, Y.; Ma, S.; Aafer, Y.; Lee, W.-C.; Zhai, J.; Wang, W.; and Zhang, X. 2018. Trojaning attack on neural networks. In *NDSS Symposium*.
- Maas, A. L.; Qi, P.; Xie, Z.; Hannun, A. Y.; Lengerich, C. T.; Jurafsky, D.; and Ng, A. Y. 2017. Building DNN acoustic models for large vocabulary speech recognition. *Computer Speech & Language*, 41: 195–213.
- Nguyen, A.; and Tran, A. 2021. Wanet-imperceptible warping-based backdoor attack. *arXiv preprint arXiv:2102.10369*.
- Nguyen, T. A.; and Tran, A. 2020. Input-aware dynamic backdoor attack. *Advances in Neural Information Processing Systems*, 33: 3454–3464.
- Parmar, D. N.; and Mehta, B. B. 2014. Face recognition methods & applications. *arXiv preprint arXiv:1403.0485*.
- Paszke, A.; Gross, S.; Massa, F.; Lerer, A.; Bradbury, J.; Chanan, G.; Killeen, T.; Lin, Z.; Gimelshein, N.; Antiga, L.; et al. 2019. Pytorch: An imperative style, high-performance deep learning library. *Advances in neural information processing systems*, 32.
- Qi, X.; Xie, T.; Wang, J. T.; Wu, T.; Mahlouljifar, S.; and Mittal, P. 2023. Towards a proactive {ML} approach for detecting backdoor poison samples. In *32nd USENIX Security Symposium (USENIX Security 23)*, 1685–1702.
- Shafahi, A.; Huang, W. R.; Najibi, M.; Suci, O.; Studer, C.; Dumitras, T.; and Goldstein, T. 2018. Poison frogs! targeted clean-label poisoning attacks on neural networks. *Advances in neural information processing systems*, 31.

Simonyan, K.; and Zisserman, A. 2014. Very deep convolutional networks for large-scale image recognition. *arXiv preprint arXiv:1409.1556*.

Singh, S. P.; and Jaggi, M. 2020. Model fusion via optimal transport. *Advances in Neural Information Processing Systems*, 33: 22045–22055.

Theus, A.; Geimer, O.; Wicke, F.; Hofmann, T.; Anagnostidis, S.; and Singh, S. P. 2024. Towards Meta-Pruning via Optimal Transport. *arXiv preprint arXiv:2402.07839*.

Wang, B.; Yao, Y.; Shan, S.; Li, H.; Viswanath, B.; Zheng, H.; and Zhao, B. Y. 2019. Neural cleanse: Identifying and mitigating backdoor attacks in neural networks. In *2019 IEEE symposium on security and privacy (SP)*, 707–723. IEEE.

Wei, S.; Zhang, M.; Zha, H.; and Wu, B. 2023. Shared adversarial unlearning: Backdoor mitigation by unlearning shared adversarial examples. *Advances in Neural Information Processing Systems*, 36: 25876–25909.

Wu, B.; Chen, H.; Zhang, M.; Zhu, Z.; Wei, S.; Yuan, D.; and Shen, C. 2022. Backdoorbench: A comprehensive benchmark of backdoor learning. In *NeurIPS Datasets and Benchmarks Track*.

Wu, B.; Liu, L.; Zhu, Z.; Liu, Q.; He, Z.; and Lyu, S. 2023. Adversarial machine learning: A systematic survey of backdoor attack, weight attack and adversarial example. *arXiv preprint arXiv:2302.09457*, 1.

Wu, D.; and Wang, Y. 2021. Adversarial neuron pruning purifies backdoored deep models. *Advances in Neural Information Processing Systems*, 34: 16913–16925.

Xie, T.; Qi, X.; He, P.; Li, Y.; Wang, J. T.; and Mittal, P. 2024. BaDExpert: Extracting Backdoor Functionality for Accurate Backdoor Input Detection. In *The Twelfth International Conference on Learning Representations*.

Yan, Z.; Li, S.; Zhao, R.; Tian, Y.; and Zhao, Y. 2023. DHBE: data-free holistic backdoor erasing in deep neural networks via restricted adversarial distillation. In *Proceedings of the 2023 ACM Asia Conference on Computer and Communications Security*, 731–745.

Zeng, Y.; Chen, S.; Park, W.; Mao, Z. M.; Jin, M.; and Jia, R. 2021a. Adversarial unlearning of backdoors via implicit hypergradient. *arXiv preprint arXiv:2110.03735*.

Zeng, Y.; Park, W.; Mao, Z. M.; and Jia, R. 2021b. Rethinking the backdoor attacks’ triggers: A frequency perspective. In *ICCV*.

Zhao, S.; Ma, X.; Zheng, X.; Bailey, J.; Chen, J.; and Jiang, Y.-G. 2020. Clean-label backdoor attacks on video recognition models. In *Proceedings of the IEEE/CVF conference on computer vision and pattern recognition*, 14443–14452.

Zheng, R.; Tang, R.; Li, J.; and Liu, L. 2022. Data-free backdoor removal based on channel lipschitzness. In *European Conference on Computer Vision*, 175–191. Springer.

Zhu, M.; Wei, S.; Shen, L.; Fan, Y.; and Wu, B. 2023. Enhancing fine-tuning based backdoor defense with sharpness-aware minimization. In *Proceedings of the IEEE/CVF International Conference on Computer Vision*, 4466–4477.

Appendix

Algorithm Outline

The OTBR defense method we propose in this paper can be summarized in Algorithm 2. By inputting a backdoored model θ_{bd} and numerous hyperparameters, we aim to obtain a repaired clean model in a data-free manner. Specifically, we generate a random dataset \mathcal{D}_r (line 2) to conduct random unlearning on θ_{bd} (line 3). Then, we calculate the NWCs (line 4) and use them to obtain a data-free model θ_{pn} by pruning (line 5). After obtaining the pruned model and the NWCs, we conduct Algorithm 1 with the original backdoored model θ_{bd} and some hyperparameters λ and p (line 7). The clean model is obtained from Algorithm 1.

Algorithm 2: OTBR method

Input: Backdoored model θ_{bd} , random noise size $[A, H, W]$, batch size B , largest class label G , the number of iterative steps I , pruning ratio γ , balance coefficient λ , the first pruned layer p

Output: Clean model θ^*

- 1: /* **Stage 1: Random-Unlearning NWC Pruning** */
 - 2: $\mathcal{D}_r \leftarrow$ Randomly generate $I \times B$ pairs of noise data.
 - 3: $\theta_{ul} \leftarrow$ Unlearn θ_{bd} by equation (1) using \mathcal{D}_r .
 - 4: Calculate NWCs by equation (2) using θ_{ul} and θ_{bd} .
 - 5: $\theta_{pn} \leftarrow$ Prune the largest- γ NWC neurons of θ_{bd} .
 - 6: /* **Stage 2: Pruned-to-Backdoored OT-based Fusion** */
 - 7: $\theta^* \leftarrow$ Conduct Algorithm 1 with input $(\theta_{pn}, \theta_{bd}, NWCs, \lambda, p)$.
-

Complementary Details of Related Work

Backdoor Defense. As illustrated in the **Related Work** section, backdoor defenses can be categorized into three main types: pre-training, in-training, and post-training defenses. Here, we provide more details on the pre-training and in-training defenses. **(1) Pre-training Defense.** This type of defense aims to detect and remove poisoned samples from the training dataset before the model training phase begins. For instance, AC (Chen et al. 2018) uses abnormal activation clustering of the target class to identify and filter out poisoned samples, while Confusion Training (Qi et al. 2023) trains a poisoned model to detect and filter out the poisoned samples that only fit the model’s specific characteristics. **(2) In-training Defense.** In this type, defenders focus on the model-training phase, where they have access to both the poisoned training dataset and the training process. ABL (Li et al. 2021b) exploits the observation that loss reduction for poisoned data is faster than that for clean data during the initial training phases, enabling it to isolate and unlearn the poisoned samples; Similarly, D-ST/D-BR (Chen, Wu, and Wang 2022) identifies a significant sensitivity of poisoned data during the feature representation transformations; DBD (Huang et al. 2022) separates the training of the feature extractor and classifier using different learning techniques to avoid learning the trigger-label correlation.

Table 3: Summary of datasets used in our experiments.

Datasets	# Input Size	# Classes	# Training Images	# Testing Images
CIFAR-10	$3 \times 32 \times 32$	10	50,000	10,000
Tiny ImageNet	$3 \times 64 \times 64$	200	100,000	10,000
CIFAR-100	$3 \times 32 \times 32$	100	50,000	10,000

Implementation Details

Computing Infrastructure. All experiments are conducted on a server with 8 *NVIDIA RTX A6000* GPUs and a *Intel(R) Xeon(R) Gold 6226R* CPU. These experiments were successfully executed using less than 49G of memory on a single GPU card. The system version is *Ubuntu 20.04.6 LTS*. We use PyTorch (Paszke et al. 2019) for implementation.

Dataset Details. Our experiments are conducted on *CIFAR-10* (Krizhevsky, Hinton et al. 2009), *Tiny ImageNet* (Le and Yang 2015), and *CIFAR-100* (Krizhevsky, Hinton et al. 2009). We provide a detailed summary of these three datasets in Table 3.

Attack Details. We conduct comprehensive evaluations using seven SOTA backdoor attacks, including BadNets (Gu et al. 2019), Blended (Chen et al. 2017), Input-aware (Nguyen and Tran 2020), LF (Zeng et al. 2021b), SSBA (Li et al. 2021a), Trojan (Liu et al. 2018) and WaNet (Nguyen and Tran 2021). All attacks are conducted using the default settings in BackdoorBench (Wu et al. 2022). Figure 7 shows examples of all seven attacks on CIFAR-10. Specifically, for BadNets, a 3×3 white square is patched at the bottom-right corner of the images for CIFAR-10 and CIFAR-100, while a 6×6 white square is used for Tiny ImageNet. For Blended, a Hello-Ketty image is blended into the images with a transparent ratio of 0.2. We choose a 10% poisoning ratio and the 0th label as the default settings to conduct attacks and test all defenses, following previous works (Zhu et al. 2023; Wei et al. 2023). Other poisoning ratios of 5%, 1%, 0.5%, and 0.1% are used only for testing our proposed method.

Defense Details. We compare our proposed OTBR method with six SOTA defense methods, including Fine-pruning (FP) (Liu, Dolan-Gavitt, and Garg 2018), NAD (Li et al. 2021c), ANP (Wu and Wang 2021), i-BAU (Zeng et al. 2021a), RNP (Li et al. 2023b), and CLP (Zheng et al. 2022). Note that only CLP can be conducted in a data-free manner similar to OTBR, while the other five defenses are all data-dependent. Therefore, we follow the common setting in the post-training scenario, providing 5% clean data for those methods. The learning rate for all methods is set to 10^{-2} , and the batch size is set to 256. For RNP, the clean data ratio is adjusted to 0.5% since we found that RNP did not perform well with the 5% setting. For OTBR, we set the number of iterative steps I to 20 during random unlearning. The generated noise conditions are similar to CIFAR-10, with image shapes set to $[3, 32, 32]$ and the largest label G set to the out-

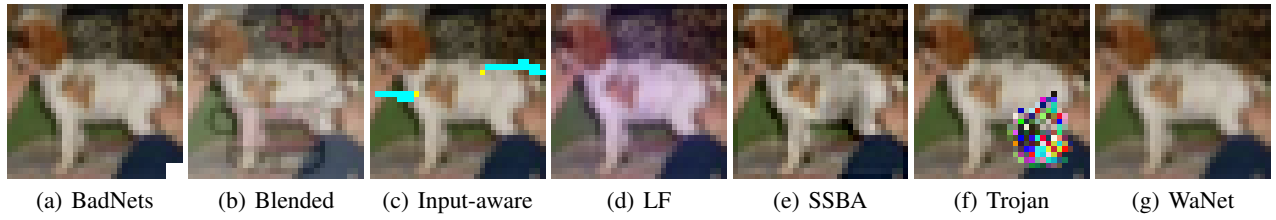


Figure 7: Examples of all seven backdoor attacks on CIFAR-10 used in our experiments.

Table 4: Operation time of each step on OTBR and CLP.

Defense	Defense Step	CIFAR-10	Tiny ImageNet
OTBR	Random Unlearning + Pruning	1.96s	0.91s
	OT + Fusion	1.16s	1.29s
CLP	Calculate UCLC + Pruning	8.04s	8.09s

put dimension of the backdoored model. The default pruning ratio γ is set to 5%, and the balance coefficient λ is set to 0.5.

More Experiments

Computational Cost. We now analyze the computational cost of our proposed OTBR in terms of runtime on CIFAR-10 and Tiny ImageNet. The operation time for each defense step of OTBR and CLP is illustrated in Table 4. We observe that for OTBR, both Stage 1 (Random Unlearning + Pruning) and Stage 2 (OT + Fusion) are highly efficient, with runtimes of less than 2 seconds. However, CLP, as the compared data-free defense, is much slower than OTBR in calculating the UCLC (*Upper bound of the Channel Lipschitz Constant*) and in pruning, e.g., $8.04s > (1.96s + 1.16s)$ in CIFAR-10. The reason is that CLP needs to calculate each neuron’s UCLC individually, while our OTBR can calculate NWC and conduct OT-based Fusion layer by layer.

Performance Under Different Poisoning Ratios. To evaluate the effectiveness of OTBR under different poisoning ratios, we test the BadNets attack on both CIFAR-10 and Tiny ImageNet datasets. The testing range includes poisoning ratios of 10%, 5%, 1%, 0.5%, and 0.1%. It is important to note that a smaller poisoning ratio results in a more hidden attack. As shown in Table 5, OTBR consistently succeeds in defense regardless of the poisoning ratio.

Performance on Different Model Structures. We evaluate the effectiveness of OTBR on different model structures except for the default PreAct-ResNet18. Specifically, we consider the VGG19-BN (Simonyan and Zisserman 2014) and ResNet18 (He et al. 2016a) models, comparing OTBR with CLP on CIFAR-10. The results, shown in Table 6, reveal that OTBR successfully defends against various attacks on both models, while CLP fails to defend against Trojan in VGG19-BN. This validates the effectiveness of OTBR across different model structures.

Further Analysis

Why Can Random-Unlearning NWCs Expose Backdoors? To answer this question, we take a close look at the unlearning process using both random data and clean data as inputs. Figure 9 compares the changes in ACC and ASR between clean unlearning and random unlearning. We observe that during the first few iterative steps, unlearning random noise adversely affects both ACC and ASR, while unlearning clean data only declines ACC, which is intuitively reasonable. However, after more unlearning steps, the performance for both types of unlearning converges, resulting in high ASR and low ACC. From the above derivation, we deduce that both types of unlearning optimization achieve similar results after a certain number of iterative steps, which suggests similar weight-change behavior in neurons. Therefore, by replacing clean unlearning with random unlearning, we can also expose the backdoor-related neurons using NWCs, as demonstrated in (Lin et al. 2024).

Observations in Activations. The activation comparisons between the backdoored model and the final fused model are shown in Figure 8. The left subfigure represents poisoned inputs, while the right subfigure represents clean inputs. We observe that neurons with high-NWCs, which are more backdoor-related, experience a similar decrease in activation levels for both poisoned and clean inputs, while a significant drop occurs for poisoned inputs. This indicates that the defense is successful while having a minimal impact on clean functionality.

Table 5: Performance under different poisoning ratios on BadNet (%).

Poisoning Ratio		10%		5%		1%		0.5%		0.1%	
Datasets	Metric	No Defense	Ours	No Defense	Ours	No Defense	Ours	No Defense	Ours	No Defense	Ours
CIFAR-10	ACC	91.32	90.11	92.64	89.25	93.14	89.49	93.76	91.04	93.61	90.83
	ASR	95.03	1.08	88.74	0.28	74.73	0.17	50.06	0.18	1.23	1.21
Tiny ImageNet	ACC	56.23	54.13	56.22	52.90	57.15	48.29	57.40	54.98	57.51	52.31
	ASR	100.00	0.00	99.85	0.00	95.01	0.01	91.26	1.98	33.52	2.24

Table 6: Performances of different models on CIFAR-10.

Model	Attacks	No Defense		CLP		OTBR	
		ACC	ASR	ACC	ASR	ACC	ASR
VGG19-BN	LF	83.27	93.83	81.99	14.61	80.73	18.37
	Trojan	91.57	100.00	90.56	99.70	88.06	0.11
ResNet18	BadNets	91.72	94.80	91.49	9.02	84.64	8.07
	Input-aware	91.75	92.96	91.28	1.66	91.06	2.20

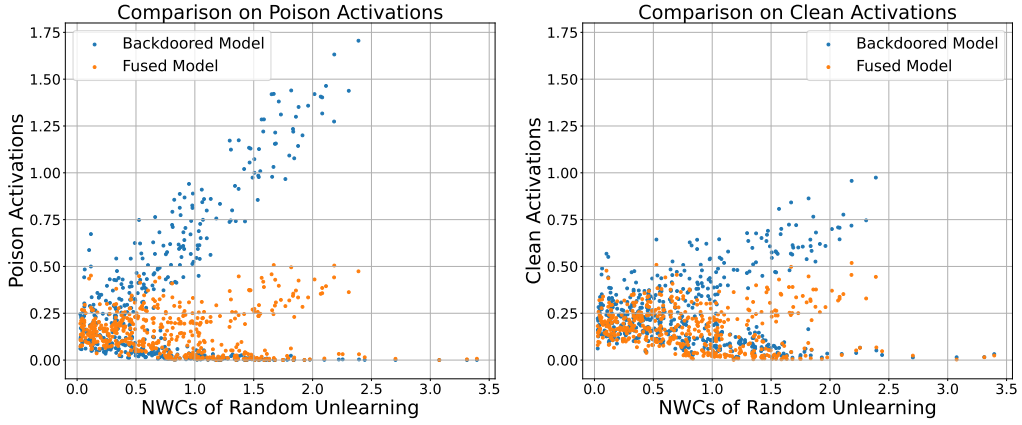


Figure 8: Illustration of neuron-level activations on backdoored and fused models. **Left:** the activations of backdoored and fused models with poisoned input; **Right:** the activations of backdoored and fused models with clean input. The last convolutional layer with *relu* activation function is used for illustration.

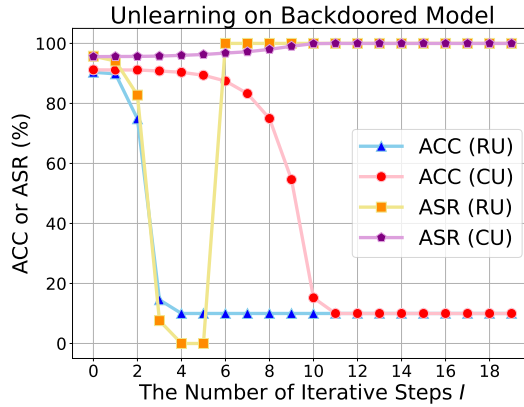


Figure 9: Comparisons of the unlearning process on clean input and random input on the backdoored model. RU: *Random Unlearning*; CU: *Clean Unlearning*.